

## Effects of electron-electron interaction and electron spin correlations on the exchange coupling in mesoscopic rings

E. Heidari Semiromi<sup>1,\*</sup> and F. Ebrahimi<sup>1,2,†</sup><sup>1</sup>*Department of Physics, Shahid Beheshti University, Evin, Tehran 19839, Iran*<sup>2</sup>*Department of Nano and Microelectronics Engineering, Shahid Beheshti University, Evin, Tehran 1983963113, Iran*

(Received 12 February 2006; published 22 May 2006)

Using the formalism of Lobo, Singwi, and Tosi (LST), we study the effect of electron-electron interaction and electron spin correlations on the indirect exchange interaction between two nuclear spins embedded in a mesoscopic metallic ring, threaded by an Aharonov-Bohm magnetic flux. We first calculate the spin local field correction and the spin-density response function of the ring in a self-consistent manner. Then, we employ the Ruderman-Kittel-Kasuga-Yosida (RKKY) theory to determine the variation of the exchange coupling as a function of the magnetic flux and the angular distance between the two nuclear spins. The LST approach predicts a reach behavior for the exchange coupling as a function of the magnetic flux. Our numerical results show that due to the electron-electron interaction and the electron spin-correlations the exchange coupling can change sign as a function of the magnetic flux, contrary to the prediction of the random phase approximation. Furthermore, the exchange coupling beside its usual oscillatory behavior acquires an oscillatory envelope which brings about strong RKKY interaction between the two nuclear spins even at far distances on the ring.

DOI: [10.1103/PhysRevB.73.195418](https://doi.org/10.1103/PhysRevB.73.195418)

PACS number(s): 71.45.Gm, 75.30.Hx, 75.30.Et

### I. INTRODUCTION

The possibility of using the two-level nature of spin- $\frac{1}{2}$  magnetic moments such as nuclear spins, to create a solid state quantum computer is a potentially revolutionary idea that has been a subject of great interest in the past few years.<sup>1-3</sup> Several spin-based quantum computers have been proposed and extensively studied.<sup>4-15</sup>

The basic unit in a quantum computer is the quantum bit (qubit), the quantum analog of the binary bit in a classical digital computer. It is essentially a controllable quantum two level system.<sup>3,16,17</sup> Quantum rings with two spin dependent impurities are suitable candidates for qubits.<sup>18,19</sup> Two nuclear spins that are embedded in a mesoscopic metallic ring, induce spin polarization in the conduction electrons of the ring and couple to each other. Such indirect coupling between nuclear spins mediated by electron spins was studied first by Ruderman-Kittel-Kasuya-Yosida.<sup>20-22</sup> The RKKY interaction plays an important role in various problems involving the interaction between localized spins embedded in metals.<sup>23,24</sup> Recent progress in semiconductor nanotechnology enables one to observe the RKKY interaction in coupled semiconductor quantum dot systems.<sup>25-27</sup>

Theoretical study of the indirect nuclear spin interaction in mesoscopic rings in the presence of a magnetic flux has increased hopes that one can use such systems for qubits. Pershin *et al.*<sup>19</sup> used the single-electron approximation, without considering the electron-electron interaction and the influence of the electron correlations, and showed that the indirect coupling of two nuclear spins embedded in a mesoscopic ring exhibits sharp maxima as a function of the magnetic field and nuclear spin positions. They proposed that mesoscopic rings have all the essential criteria for the qubits for the realization of a quantum computer.<sup>5</sup> Utsumi *et al.* have also investigated the RKKY interaction between two spins located at two quantum dots embedded in an Aharonov-Bohm (AB) ring.<sup>28</sup> Using a noninteracting ap-

proximation, they assert that by means of an external flux one can control the amplitude of the RKKY interaction, but it is not possible to change its sign. However, controlling the RKKY interaction, acting between local spins embedded in an AB ring, by an external magnetic field can be used to construct a universal quantum gate<sup>29</sup> and therefore is useful for spin-based quantum computers.<sup>30</sup>

In this paper, our main concentration is on the effect of the electron-electron interaction and the electron spin correlations on the indirect exchange coupling between two nuclear spins embedded in a mesoscopic metallic ring. We use the Lobo-Singwi-Tosi (LST) approach to study the dependence of the RKKY interaction between two nuclear spins on the nuclear spin locations and on the magnetic flux. We find that the electron-electron interaction and the electron spin correlation effects lead to a transition from ferromagnetic to antiferromagnetic coupling. This means that, contrary to the assertion of Refs. 19 and 28, the sign of indirect exchange coupling between two nuclear spins embedded in the AB ring can be changed by changing the magnetic flux. Furthermore, our numerical results predict an oscillatory envelope for the amplitude of the exchange coupling beside its usual  $2k_F$  oscillatory behavior. These effects which are due to the quasi-one-dimensionality of the AB ring and its circular geometry, can be used for the control of the RKKY interaction that is important for constructing qubits.

The organization of this paper is as follows: In Sec. II we present our model. In Sec. III the formalism of the LST approach is generalized for the AB ring by using the second quantization technique. The numerical results of the self-consistent scheme obtained in Sec. III are then used in Sec. IV to determine the dependence of the RKKY interaction on the nuclear spin locations and on the magnetic flux. Finally, a discussion and conclusions are presented in Sec. V.

### II. MODEL

Although strictly one-dimensional (1D) fermionic systems are Luttinger liquids,<sup>31-33</sup> real quasi-one-dimensional

systems due to scattering from impurities show Fermi liquid behavior.<sup>34</sup> We model the mesoscopic ring with a 1D jellium consisting of the confined electrons and uniformly distributed positive background charges with a 1D circular shape geometry, threaded by an Aharonov-Bohm (AB) magnetic flux  $\phi$ . We also assume that the ring is embedded in a dielectric medium with a dielectric constant,  $\epsilon_s$ , and the electron-electron interaction is the normal Coulomb interaction  $e^2/\epsilon_s r$ , down to the classical radius of the electron.

Choosing the  $xy$  plane as the plane of the ring and the magnetic field in the  $z$  direction, the Hamiltonian of the jellium can be written as follows:

$$\hat{H} = \hat{H}_{el} + \hat{H}_b + \hat{H}_{el-b}, \quad (1)$$

where

$$\begin{aligned} \hat{H}_{el} = & \int_0^{2\pi} R d\theta \hat{\psi}^\dagger(\theta) \hat{T}(\theta) \hat{\psi}(\theta) \\ & + \frac{1}{2} \int_0^{2\pi} R d\theta \int_0^{2\pi} R d\theta' \hat{\psi}^\dagger(\theta) \hat{\psi}^\dagger(\theta') V(\theta, \theta') \hat{\psi}(\theta') \hat{\psi}(\theta) \end{aligned} \quad (2)$$

is the Hamiltonian of the electrons,

$$\hat{H}_b = \frac{1}{2} \int_0^{2\pi} R d\theta \int_0^{2\pi} R d\theta' n(\theta) n(\theta') V(\theta, \theta') \quad (3)$$

is the energy of the positive background with particle density  $n(\theta)$ , and

$$\hat{H}_{el-b} = \int_0^{2\pi} R d\theta \int_0^{2\pi} R d\theta' n(\theta') \hat{\psi}^\dagger(\theta) V(\theta, \theta') \hat{\psi}(\theta) \quad (4)$$

is the interaction energy between the electrons and the positive background.

In Eqs. (2), (3), and (4),  $\hat{T}(\theta)$  and the  $V(\theta, \theta')$  are

$$\hat{T}(\theta) = \frac{\hbar^2}{2m^* R^2} \left( i \frac{\partial}{\partial \theta} - \varphi \right)^2 \quad (5)$$

and

$$V(\theta, \theta') = \frac{e^2}{2\epsilon_s R} \left[ \sin^2 \left( \frac{\theta - \theta'}{2} \right) + \left( \frac{r_c}{R} \right)^2 \right]^{-1/2}, \quad (6)$$

respectively. Here,  $m^*$  is the effective electron mass,  $R$  is the radius of the ring,  $\theta$  is the azimuthal angle in the polar coordinate,  $L=2\pi R$  is the circumference of the ring,  $\varphi$  is the AB flux in terms of quantum flux  $hc/e$ , and  $r_c$  is the classical radius of the electron.

In terms of the single particle eigenfunctions of the kinetic energy operator  $\hat{T}(\theta)$ , the field operators  $\hat{\psi}(\theta)$  and  $\hat{\psi}^\dagger(\theta)$  are given by

$$\hat{\psi}(\theta) = \frac{1}{\sqrt{L}} \sum_{n,\alpha} e^{in\theta} \eta_\alpha a_{n,\alpha}, \quad (7)$$

$$\hat{\psi}^\dagger(\theta) = \frac{1}{\sqrt{L}} \sum_{n,\alpha} e^{-in\theta} \eta_\alpha^\dagger a_{n,\alpha}^\dagger, \quad (8)$$

where  $a_{n,\alpha}^\dagger$ 's and  $a_{n,\alpha}$ 's are electron creation and destruction operators, respectively, with angular quantum numbers  $n=0, \pm 1, \pm 2, \dots$ , and  $\eta_\alpha$ 's for  $\alpha=1, 2$  are the spin wave functions for spin-up and spin-down along the  $z$  axis.

Using Eqs. (2)–(8) in Eq. (1), we obtain the total Hamiltonian of the ring in terms of the electron creation and destruction operators as follows:

$$\begin{aligned} \hat{H} = & \sum_{n,\alpha} \varepsilon_n(\varphi) a_{n,\alpha}^\dagger a_{n,\alpha} \\ & + \frac{1}{2L} \sum_{mnn'} \sum_{\alpha,\alpha'} V(m) a_{n+m,\alpha}^\dagger a_{n'-m,\alpha'}^\dagger a_{n',\alpha'} a_{n,\alpha} - \frac{1}{2} \frac{N^2}{L} V(0), \end{aligned} \quad (9)$$

where

$$\varepsilon_n(\varphi) = \frac{\hbar^2}{2m^* R^2} (n - \varphi)^2, \quad (10)$$

$N$  is the number of the electrons on the ring and  $V(m)$  is the  $m$ th Fourier component of the electron-electron interaction given by

$$V(m) = \frac{2e^2}{\epsilon_s} Q_{|m|+\frac{1}{2}} [1 + 2(r_c/R)^2], \quad (11)$$

where  $Q_\nu(x)$  is the second kind Legendre function.

If we separate the sum in the second term of the right-hand side of Eq. (9) into the terms  $m=0$  and  $m \neq 0$ , then the term  $m=0$  can be written as follows:

$$\frac{1}{2L} \sum_{nn'} \sum_{\alpha,\alpha'} V(0) a_{n,\alpha}^\dagger a_{n',\alpha'}^\dagger a_{n',\alpha'} a_{n,\alpha} = \frac{1}{2L} V(0) (\hat{N}^2 - \hat{N}), \quad (12)$$

where

$$\hat{N} = \sum_{n,\alpha} a_{n,\alpha}^\dagger a_{n,\alpha} \quad (13)$$

is the electron number operator.

Since  $\hat{N}$  is a constant of motion, we can substitute its eigenvalue  $N$ , i.e., the total number of the electrons on the ring. This leads to two constant terms  $\frac{N^2}{2L} V(0)$  and  $-\frac{N}{2L} V(0)$ . The latter term cancels the last term in Eq. (9), and the former term is a finite term which shifts all the energy levels of the ring by an overall constant. Ignoring this term, the Hamiltonian of the ring simplifies to

$$\begin{aligned} \hat{H} = & \sum_{n,\alpha} \varepsilon_n(\varphi) a_{n,\alpha}^\dagger a_{n,\alpha} + \frac{1}{2L} \sum_{mnn'} \sum_{\alpha,\alpha'} V(m) \\ & \times a_{n+m,\alpha}^\dagger a_{n'-m,\alpha'}^\dagger a_{n',\alpha'} a_{n,\alpha}. \end{aligned} \quad (14)$$

### III. LST FORMALISM

The Lobo-Singwi-Tosi (LST) approach is a powerful theoretical tool, going beyond the random phase approximation (RPA), in studying the spin correlation effects of an interacting electron gas. It was originally developed for three-dimensional (3D) electron gas<sup>35</sup> and subsequently applied to two-dimensional (2D)<sup>36</sup> and 1D (Ref. 37) electron gas, but has not been used for 1D mesoscopic rings. In this section we present the necessary formulas of the LST approach for an AB ring.

The noninteracting single particle Greens' function of the ring is given by

$$iG_{\alpha\beta}^0(\theta t, \theta' t') = \langle \Phi_0 | T[\hat{\psi}_{I\alpha}(\theta t) \hat{\psi}_{I\beta}^\dagger(\theta' t')] | \Phi_0 \rangle, \quad (15)$$

where the noninteracting ground state vector  $|\Phi_0\rangle$  is assumed to be normalized and the field operators of the system in the interaction picture are

$$\hat{\psi}_{I\alpha}(\theta, t) = \frac{1}{\sqrt{L}} \sum_{n=-\infty}^{+\infty} a_{n\alpha} e^{-i\omega_n(\varphi)t} e^{in\theta} \eta_\alpha, \quad (16)$$

$$\hat{\psi}_{I\alpha}^\dagger(\theta, t) = \frac{1}{\sqrt{L}} \sum_{n=-\infty}^{+\infty} a_{n\alpha}^\dagger e^{i\omega_n(\varphi)t} e^{-in\theta} \eta_\alpha^\dagger \quad (17)$$

with  $\omega_n(\varphi) = \varepsilon_n(\varphi)/\hbar$ . Substituting Eqs. (16) and (17) in Eq. (15), we obtain an expression for the single-particle Greens' function in the base's space of the kinetic energy operator as follows:

$$G_{\alpha\beta}^0(n, \omega, \varphi) = \delta_{\alpha\beta} \left[ \frac{\Theta(|k_n(\varphi)| - |k_F|)}{\omega - \omega_n(\varphi) + i\eta} + \frac{\Theta(|k_F| - |k_n(\varphi)|)}{\omega - \omega_n(\varphi) - i\eta} \right], \quad (18)$$

where  $\Theta$  is the usual unit step function,  $k_n(\varphi) = \frac{2\pi}{L}(n - \varphi)$  is the wave number associated with the angular quantum number  $n$  in the presence of the AB flux, and  $k_F = \frac{2\pi}{L}(n_F + \frac{1}{2})$  is the Fermi wave number with the Fermi angular quantum number  $n_F$ . The free-electron polarizability is defined by (Ref. 38)

$$\begin{aligned} \hbar \Pi^0(\theta t, \theta' t') &= -i G_{\alpha\beta}^0(\theta t, \theta' t') G_{\beta\alpha}^0(\theta' t', \theta t) \\ &= -2i G^0(\theta t, \theta' t') G^0(\theta' t', \theta t), \end{aligned} \quad (19)$$

where the sum over  $\alpha$  and  $\beta$  yields a factor of 2 for electrons. Using Eq. (18), the expression for the free-electron polarizability can be written as follows:

$$\begin{aligned} \Pi^0(n, \omega, \varphi) &= -\frac{2i}{\hbar L} \sum_{n'=-\infty}^{\infty} \int_{-\infty}^{\infty} \frac{d\omega'}{2\pi} \\ &\quad \times G^0(n', \omega', \varphi) G^0(n' + n, \omega' + \omega, \varphi). \end{aligned} \quad (20)$$

Carrying the integration over the frequency we obtain

$$\begin{aligned} \Pi^0(n, \omega, \varphi) &= \frac{2}{\hbar L} \sum_{m=-\infty}^{+\infty} \left[ \frac{\Theta(|k_F| - |k_m(\varphi)|) \Theta(|k_{m+n}(\varphi)| - |k_F|)}{\omega - [\omega_{m+n}(\varphi) - \omega_m(\varphi)] + i\eta} \right. \\ &\quad \left. - \frac{\Theta(|k_F| - |k_m(\varphi)|) \Theta(|k_{m-n}(\varphi)| - |k_F|)}{\omega + [\omega_{m-n}(\varphi) - \omega_m(\varphi)] - i\eta} \right], \end{aligned} \quad (21)$$

where the summation is over the angular quantum numbers. It is obvious that only those angular quantum numbers that make the unit step functions in the numerator simultaneously nonzero contribute to the sum. Following the idea of LST, using the free electron polarizability,  $\Pi^0(n, \omega, \varphi)$ , the spin-density response function for the mesoscopic ring can be written as (Ref. 39) follows:

$$\chi^s(n, \omega, \varphi) = -g^2 \mu_B^2 \frac{\Pi^0(n, \omega, \varphi)}{1 - I(n, \varphi) \Pi^0(n, \omega, \varphi)}, \quad (22)$$

where  $g$  is the Lande factor,  $\mu_B$  is the Bohr magneton and

$$I(n, \varphi) = V(n) \tilde{G}(n, \varphi) \quad (23)$$

is the spin-antisymmetric effective potential.

In Eq. (22),  $\tilde{G}(n, \varphi)$  is the static spin local-field correction arising from the short range Coulomb correlation and exchange-correlation effects for the spin-density response that is related to the magnetic structure factor,  $\tilde{S}(n, \varphi)$ , by

$$\tilde{G}(n, \varphi) = \frac{1}{N} \sum_{m=-\infty}^{\infty} \frac{mV(m)}{nV(n)} [\tilde{S}(n-m, \varphi) - 1], \quad (24)$$

where  $n_0 = \frac{N}{L}$  is the electron gas density. The magnetic structure factor,  $\tilde{S}(n, \varphi)$ , is related to the dynamic spin-density response function by the fluctuation-dissipation theorem as follows:

$$\tilde{S}(n, \varphi) = \frac{\hbar}{\pi n_0 g^2 \mu_B^2} \int_0^\infty d\omega \text{Im}[\chi^s(n, \omega, \varphi)], \quad (25)$$

where  $\text{Im}[\chi^s(n, \omega, \varphi)]$ , the imaginary part of the dynamic spin-density response function, can be written in terms of the free electron susceptibility,  $\Pi^0(n, \omega, \varphi)$ , as

$$\text{Im}[\chi^s(n, \omega)] = -\frac{g^2 \mu_B^2}{I(n, \varphi)} \text{Im} \left[ \frac{1}{1 - I(n, \varphi) \Pi^0(n, \omega)} \right]. \quad (26)$$

Therefore, we have

$$\tilde{S}(n, \varphi) = -\frac{\hbar}{\pi n_0 I(n, \varphi)} \int_0^\infty d\omega \text{Im} \left[ \frac{1}{1 - I(n, \varphi) \Pi^0(n, \omega, \varphi)} \right]. \quad (27)$$

Using the relation

$$\begin{aligned} &\text{Im} \left[ \frac{1}{1 - I(n, \varphi) \Pi^0(n, \omega, \varphi)} \right] \\ &= \pi \delta(1 - I(n, \varphi) \Pi^0(n, \omega, \varphi)) \\ &= \pi \sum_{\omega_0} \left| \frac{\partial}{\partial \omega} (1 - I(n, \varphi) \Pi^0(n, \omega, \varphi)) \right|_{\omega=\omega_0}^{-1} \delta(\omega - \omega_0) \end{aligned} \quad (28)$$

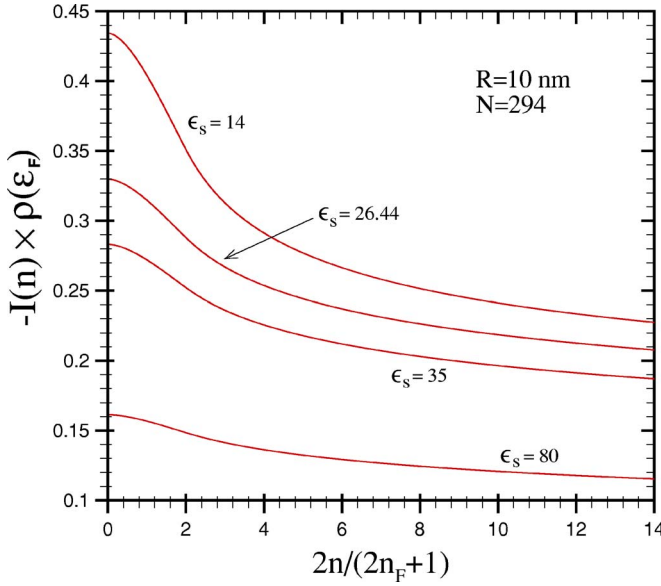


FIG. 1. (Color online) Spin-antisymmetric effective potential,  $I(n)$ , vs angular quantum number,  $n$ , for various  $\epsilon_s$ .

we can write the magnetic structure factor,  $\tilde{S}(n, \varphi)$ , as follows:

$$\tilde{S}(n, \varphi) = \frac{-\hbar}{n_0 I(n, \varphi)} \sum_{\omega_0} \left| \frac{\partial}{\partial \omega} (1 - I(n, \varphi) \Pi^0(n, \omega, \varphi)) \right|_{\omega=\omega_0}^{-1}. \quad (29)$$

With a self-consistent calculation of Eqs. (23), (24), and (29), we can obtain the spin-antisymmetric effective potential,  $I(n, \varphi)$ , the magnetic structure factor,  $\tilde{S}(n, \varphi)$ , and the static spin-density response function,  $\chi^s(n, \varphi)$ .

#### IV. RKKY INTERACTION

Now, let us consider two nuclear spins embedded in the ring. To calculate the RKKY interaction between the nuclear spins mediated by conductance electrons of the ring, we suppose that the two nuclear spins are located at positions  $\theta_1$  and  $\theta_2$ . The exchange interaction Hamiltonian between the nuclear spins and the conductance electrons of the ring is

$$H_{int} = -J_0 \sum_{i=1}^2 \int_{-\pi}^{\pi} d\theta \delta(\theta - \theta_i) \vec{s}(\theta) \cdot \vec{S}(\theta_i), \quad (30)$$

where  $J_0$  is the exchange integral,  $\vec{s}$  is the electron spin, and  $\vec{S}$  is the nuclear spin. The effective magnetic field produced by one of the nuclear spins is

$$\vec{H}_{eff} = -\frac{J_0}{g\mu_B} \delta(\theta - \theta_1) \vec{S}(\theta_1). \quad (31)$$

Using the linear response theory, the magnetization induced in the electron gas by this effective field can be written as follows:

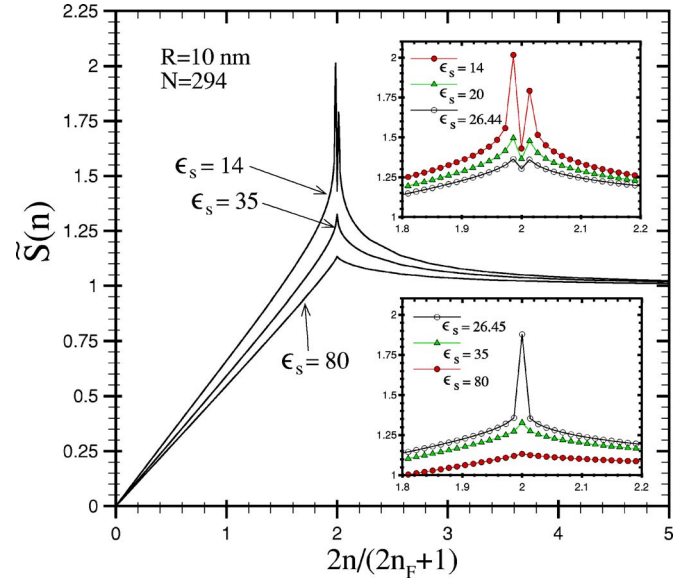


FIG. 2. (Color online) Magnetic structure factor,  $\tilde{S}(n)$ , vs angular quantum number,  $n$ , for various  $\epsilon_s$ .

$$\vec{M}(\theta) = -\frac{J_0}{2\pi g\mu_B} \sum_{n=-\infty}^{+\infty} \chi^s(n, \varphi) \vec{S}(\theta_1) e^{in(\theta - \theta_1)}, \quad (32)$$

where  $\chi^s(n, \varphi)$  is the static spin-density response function of the ring in the presence of the AB flux,  $\varphi$ .

The exchange interaction energy between the two nuclear spins in terms of the induced magnetization,  $\vec{M}(\theta)$ , has the form

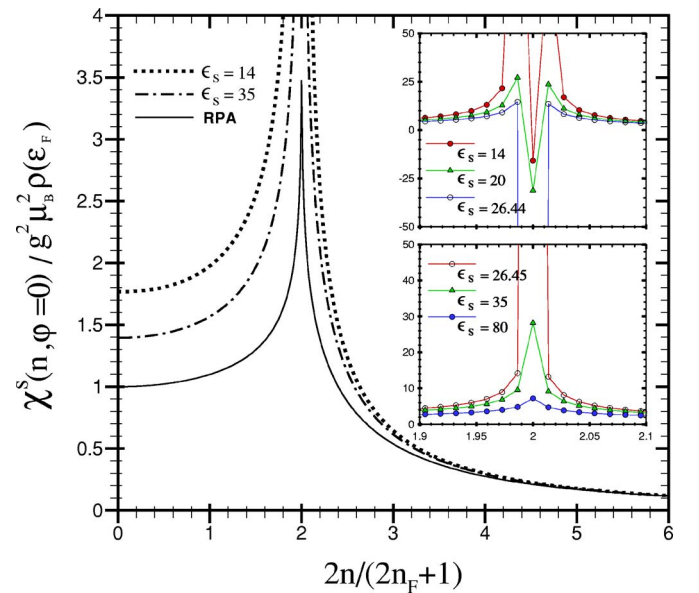


FIG. 3. (Color online) Static spin-density response function as a function of angular quantum number,  $n$ , for various  $\epsilon_s$  in the absence of the external magnetic flux. The solid line shows the static spin-density response function in RPA. The parameters of the ring are  $N=294$  and  $R=10$  nm.

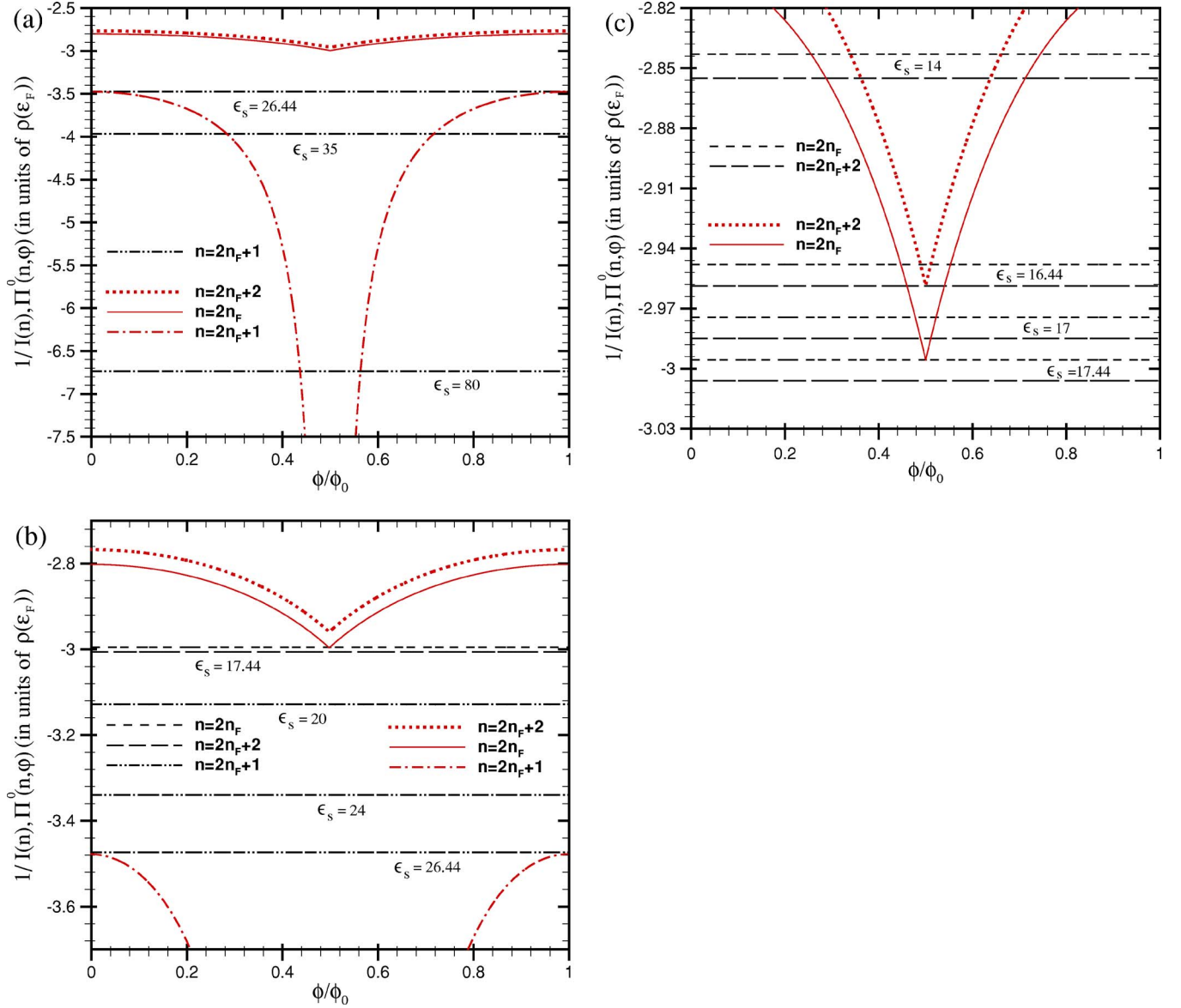


FIG. 4. (Color online) Inverse of the effective potential,  $1/I(n)$ , for  $n=2n_F+1$  (dash-dot-dotted lines),  $n=2n_F$  (dashed lines), and  $2n_F+2$  (long dashed lines), and the free-electron polarizability,  $\Pi^0(n, \varphi)$ , for  $n=2n_F+1$  (dash-dot-dotted line),  $n=2n_F$  (solid line), and  $2n_F+2$  (dotted line) are depicted as functions of flux,  $\varphi$ , to determine the intersections of this functions in the intervals (a)  $\epsilon_s > 26.44$ , (b)  $17.44 < \epsilon_s < 26.44$ , and (c)  $14 < \epsilon_s < 17.44$ . The parameters of the ring are  $N=294$  and  $R=10$  nm.

$$E = \frac{J_0}{g\mu_B} \vec{M}(\theta_2) \cdot \vec{S}(\theta_1). \quad (33)$$

Using Eq. (32), we have

$$E = \frac{-J_0^2}{2\pi^2 g^2 \mu_B^2} \sum_{n=-\infty}^{+\infty} \chi^s(n, \varphi) \vec{S}(\theta_1) \cdot \vec{S}(\theta_2) e^{in(\theta_2 - \theta_1)} \quad (34)$$

or

$$E = \frac{-J_0^2}{2\pi^2 g^2 \mu_B^2} F(\theta, \varphi) \vec{S}_1 \cdot \vec{S}_2, \quad (35)$$

where  $\theta = \theta_2 - \theta_1$  and  $F(\theta, \varphi)$  is

$$F(\theta, \varphi) = \sum_{n=-\infty}^{+\infty} \chi^s(n, \varphi) e^{in\theta} = \chi^s(0, \varphi) + 2 \sum_{n=1}^{+\infty} \chi^s(n, \varphi) \cos(n\theta). \quad (36)$$

Equation (36) shows the relation between the Fourier transform of the static spin-density response function of the ring and the space dependence of the indirect exchange coupling,  $F(\theta, \varphi)$ , between the two nuclear spins due to the conduction electrons of the ring.<sup>40</sup>

## V. DISCUSSION AND CONCLUSIONS

With a self-consistent calculation of Eqs. (23), (24), and (29) for  $N=294$  electrons on the ring with the radius

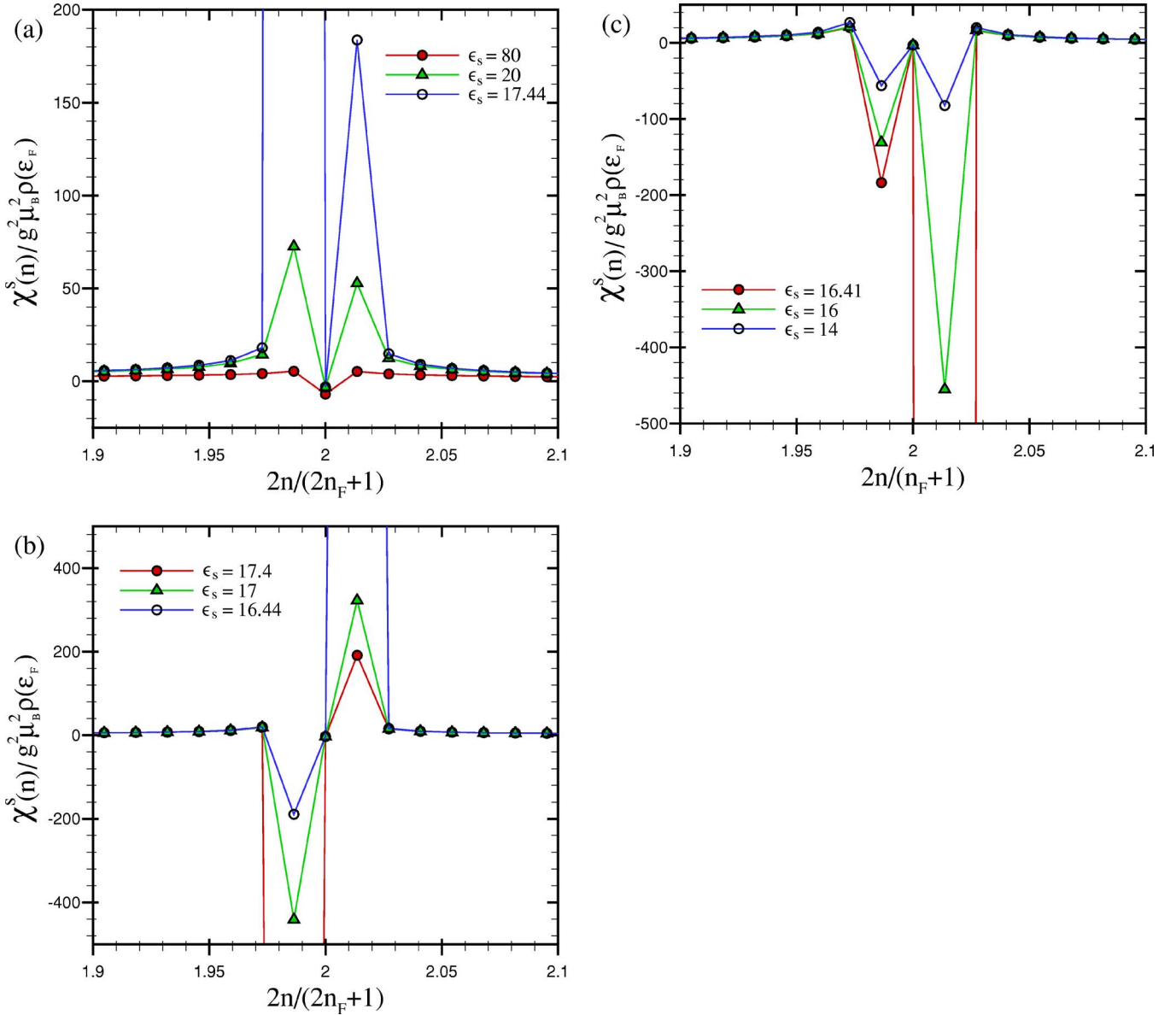


FIG. 5. (Color online) Static spin-density response function depicted as a function of angular quantum number,  $n$ , for various  $\epsilon_s$  in the presence of the external magnetic flux,  $\varphi=0.499$ , (a)  $\epsilon_s > 17.44$ , (b)  $16.44 < \epsilon_s < 17.44$ , and (c)  $14 < \epsilon_s < 16.44$ . The parameters of the ring are  $N=294$  and  $R=10$  nm.

$R=10$  nm and the density of states at the Fermi energy  $\rho(\epsilon_F) = 2m^* / \pi \hbar^2 k_F$ , we obtain the spin-antisymmetric effective potential,  $I(n)$ , the magnetic structure factor,  $\tilde{S}(n)$ , and the static spin-density response function,  $\chi^s(n, \varphi)$ , of the ring in the presence of the AB flux. We find that the structure function and consequently the spin-antisymmetric effective potential are independent of the external magnetic flux. This is due to the fact that according to Eq. (29), the magnetic structure factor is related to the slope of the denominator of the dynamic spin-density response function in Eq. (22) at its poles which is independent of the external magnetic flux. Physically, this means that the probability of finding two electrons on the ring at angular separation  $\theta$ ; i.e., the spin-antisymmetric pair correlation function  $\tilde{g}(\theta)$ , is independent of the AB flux. In Figs. 1 and 2, we have plotted  $I(n)$  and

$\tilde{S}(n)$ , respectively, for different values of the dielectric constant  $\epsilon_s$ .

The behavior of the static spin-response function of the ring in the absence of the AB flux is shown in Fig. 3 for different values of  $\epsilon_s$ . The peaks close and at  $2n_F+1$  in Figs. 2 and 3 are the characteristic of 1D systems,<sup>37,39</sup> which in the ring geometries they occur not only at  $2n_F+1$  but also at the angular quantum numbers close to  $2n_F+1$ , depending on the strength of the electron-electron interaction and the spin-correlations. We will see that this resonance behavior of the static spin response function at  $2n_F+1$  and angular quantum numbers close to it, modifies the behavior of the RKKY interactions when going beyond RPA.

We now consider the behavior of the static spin response function in the presence of the AB flux

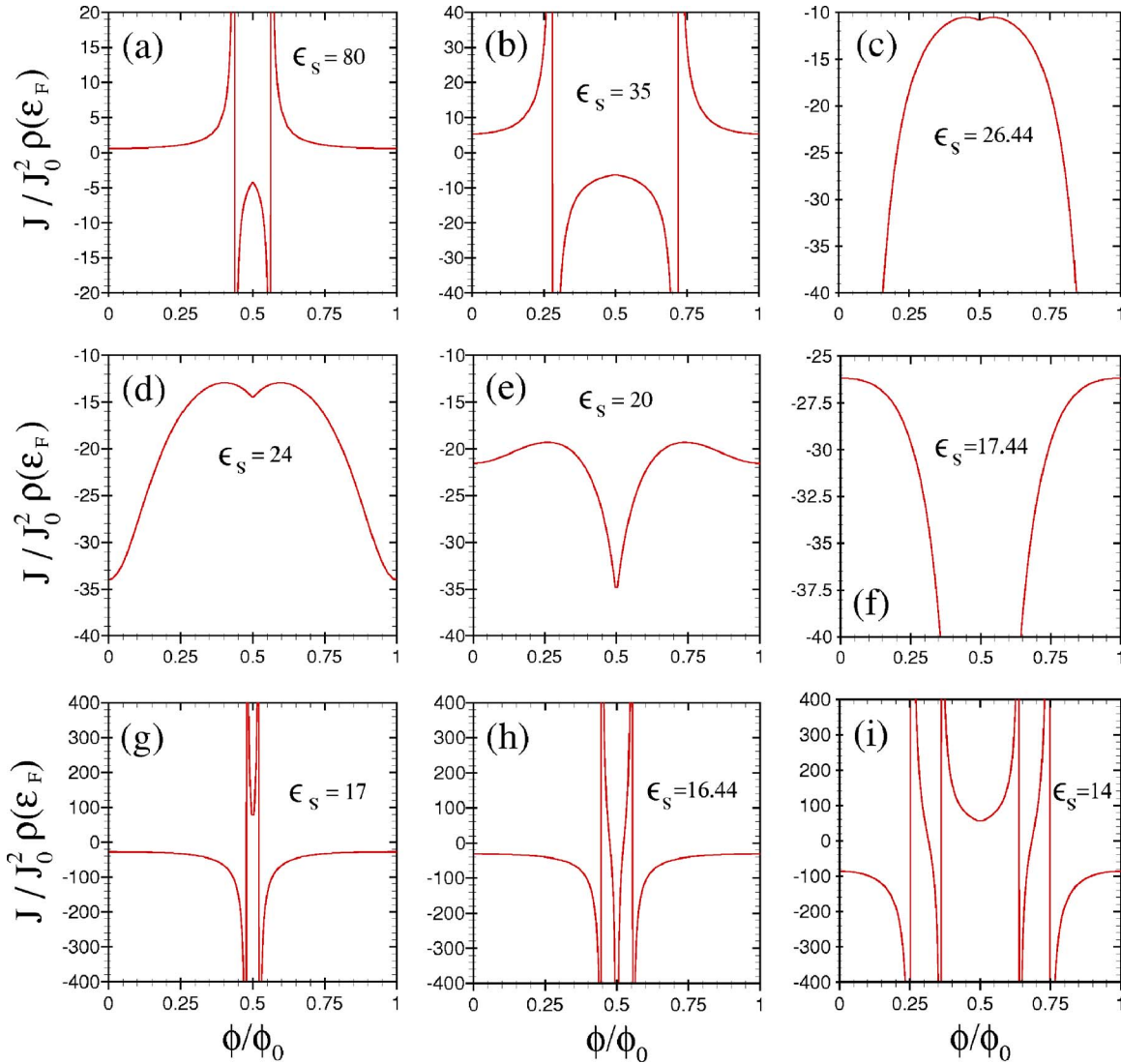


FIG. 6. (Color online) Indirect exchange coupling  $J$  as a function of the external magnetic flux  $\varphi$ , for nine dielectric constants  $\epsilon_s$ . First, (a)  $\epsilon_s=80$ , (b)  $\epsilon_s=35$ , and (c)  $\epsilon_s=26.44$  for  $\epsilon_s > 26.44$ . Next, (d)  $\epsilon_s=24$ , (e)  $\epsilon_s=20$ , and (f)  $\epsilon_s=17.44$  for  $17.44 < \epsilon_s < 26.44$ . Finally, (g)  $\epsilon_s=17$ , (h)  $\epsilon_s=16.44$ , and (i)  $\epsilon_s=14$  for  $14 < \epsilon_s < 17.44$ . The parameters of the ring are  $N=294$  and  $R=10$  nm and the angular distance between the two nuclear spins is  $\theta=\pi$ .

$$\chi^s(n, \varphi) = -g^2 \mu_B^2 \frac{\Pi^0(n, \varphi)}{1 - I(n) \Pi^0(n, \varphi)}, \quad (37)$$

by investigating its denominator in more details. In Fig. 4, we have plotted the free electron polarizability,  $\Pi^0(n, \varphi)$ , and the inverse of the effective potential,  $1/I(n)$ , as a function of the flux  $\varphi$  for the angular quantum numbers  $2n_F$ ,  $2n_F+1$ , and  $2n_F+2$ . The function  $1/I(n)$ , which is independent of the flux, behaves as a constant and is shown by horizontal lines for different values of  $\epsilon_s$ . As can be seen in Fig. 4(a) or 4(b), in the absence of the external flux ( $\varphi=0$ ), the denominator in Eq. (37) goes to zero for  $n=2n_F+1$  and  $\epsilon_s \approx 26.44$ , but the right and left limits of  $\chi^s(n, \varphi)$  are different, so we have a transition from ferromagnetic to antiferromagnetic (Fig. 3).

In the presence of the AB flux, for example  $\phi \approx 0.5$  in Fig. 4(c), the denominator in Eq. (37) goes to zero for two different values of  $n$  and  $\epsilon_s$ , one for  $n=2n_F$  and  $\epsilon_s \approx 17.44$  and the

other for  $n=2n_F+2$  and  $\epsilon_s \approx 16.44$ . In Fig. 5, we have shown the behavior of the static spin response function of the system for  $\phi \approx 0.5$  as a function of the angular quantum numbers close to  $2n_F+1$ . In terms of the strength of the spin antisymmetric effective potential or  $\epsilon_s$ , there are three different intervals according to which we can discuss the behavior of the static spin response function at the angular quantum numbers  $2n_F$  and  $2n_F+2$ :

(i) For  $\epsilon_s > 17.44$ , the system responds ferromagnetically at both  $2n_F$  and  $2n_F+2$  modes ( $\chi^s > 0$ ), Fig. 5(a). In this interval with decreasing  $\epsilon_s$ , the  $2n_F$  mode goes to infinity and the  $2n_F+2$  mode goes to a large finite value, therefore the system responds ferromagnetically as  $\epsilon_s \rightarrow 17.44^+$ .

(ii) For  $16.44 < \epsilon_s < 17.44$ , according to Fig. 5(b), the system responds antiferromagnetically at  $2n_F$  and ferromagnetically at  $2n_F+2$ . In this interval with decreasing  $\epsilon_s$ , the  $2n_F$  mode goes to lower values and the  $2n_F+2$  mode goes to higher values. Therefore the system responds antiferromag-

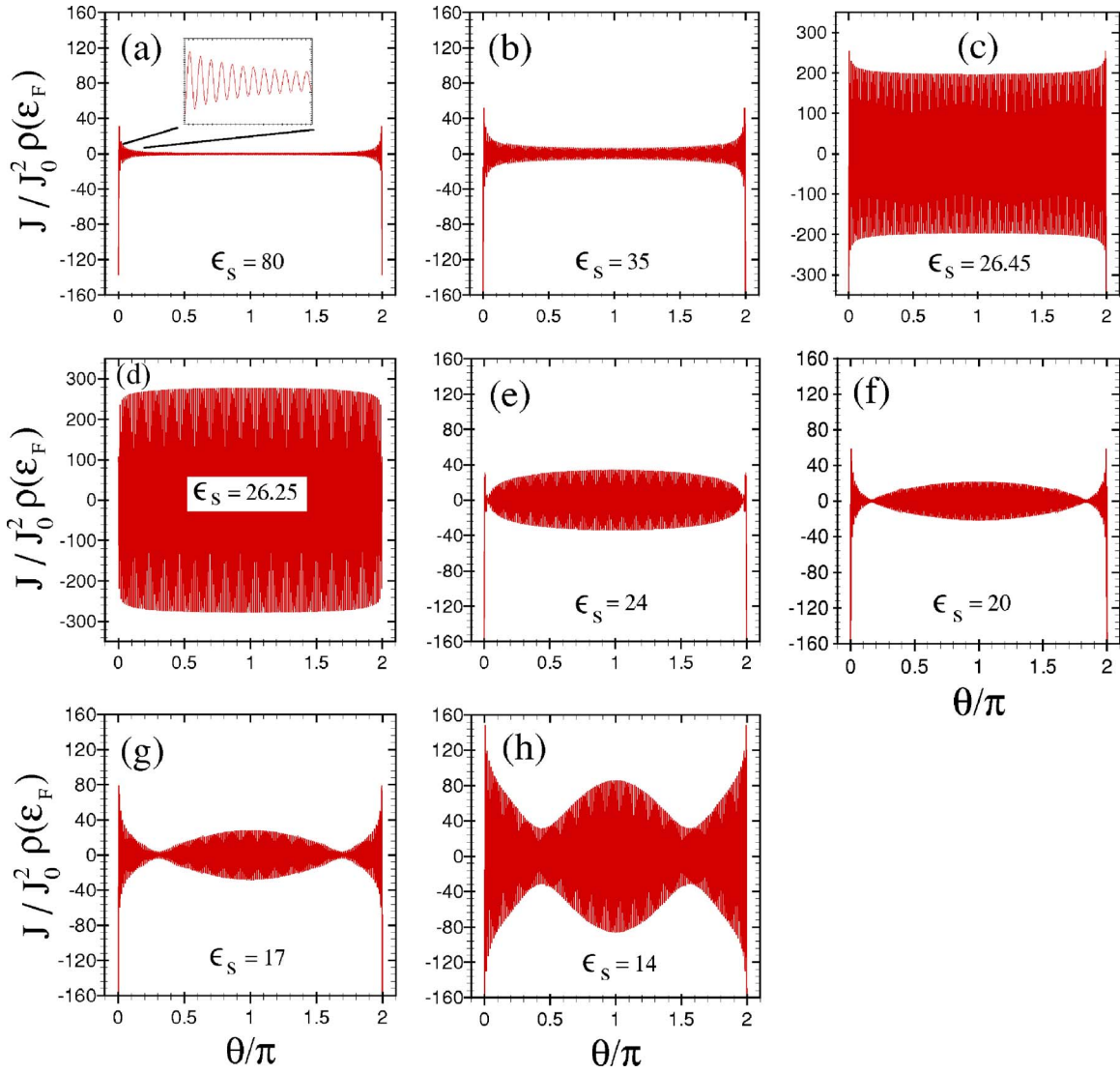


FIG. 7. (Color online) Indirect exchange coupling  $J$  vs angular distance  $\theta$ , between the two nuclear spins in the absence of the external magnetic flux, for eight dielectric constants,  $\epsilon_s$ . First, (a)  $\epsilon_s=80$ , (b)  $\epsilon_s=35$ , and (c)  $\epsilon_s=26.45$  for  $\epsilon_s > 26.44$ . Second, (d)  $\epsilon_s=26.25$ , (e)  $\epsilon_s=24$ , (f)  $\epsilon_s=20$ , (g)  $\epsilon_s=17$ , and (h)  $\epsilon_s=14$  for  $14 < \epsilon_s < 26.44$ . The parameters of the ring are  $N=294$  and  $R=10$  nm.

netically for  $\epsilon_s \rightarrow 17.44^-$  and ferromagnetically for  $\epsilon_s \rightarrow 16.44^+$ .

(iii) For  $14 < \epsilon_s < 16.44$ , the system responds antiferromagnetically at both  $2n_F$  and  $2n_F+2$  modes ( $\chi^s < 0$ ), Fig. 5(c). In this interval with decreasing  $\epsilon_s$ , the modes  $2n_F$  and  $2n_F+2$  go to finite lower values. By increasing  $\epsilon_s$  in this interval, the  $2n_F$  mode goes to a large finite value but  $2n_F+2$  mode goes to infinity and the system responds antiferromagnetically as  $\epsilon_s \rightarrow 16.44^-$ .

Using Eqs. (35) and (36) we have investigated the behavior of the RKKY interaction as a function of the external magnetic flux. The magnetic flux dependence of the RKKY interaction has been shown in Fig. 6 for various  $\epsilon_s$  in the LST approximation for the two nuclear spins at the angular separation  $\theta=\pi$ .

In RPA, the indirect coupling of the two nuclear spins exhibits sharp maxima at the half-integer values of the external flux,  $\varphi$ ,<sup>19</sup> and the two nuclear spins couple together antiferromagnetically so that there is no change in the sign of

the exchange coupling. Contrary to the RPA, the LST approach predicts transitions from ferromagnetic to antiferromagnetic coupling and vice versa between the two nuclear spins embedded in the ring as a function of the magnetic flux. Depending on the spin-correlations and on the strength of the electron-electron interaction which in turn is determined by the strength of the screening constant  $\epsilon_s$ , there are three intervals for which we can discuss the behavior of the exchange coupling between the two nuclear spins:

(1) For  $\epsilon_s > 26.44$ , Figs. 6(a)–6(c), transitions from antiferromagnetic to ferromagnetic coupling and vice versa between the two nuclear spins occurs at the magnetic fluxes determined by the intersections of the functions  $1/I(n)$  and  $\Pi^0(n, \varphi)$  in Fig. 4(a). In this interval with increasing  $\epsilon_s$ , the values of  $\varphi$  for which a coupling transition occurs tend to the half-integer values as seen in Fig. 4(a).

(2) For  $17.44 < \epsilon_s < 26.44$ , Figs. 6(d)–6(f), there is no coupling transition between the two nuclear spins, since according to Fig. 4(b) in this interval the functions  $1/I(n)$  and

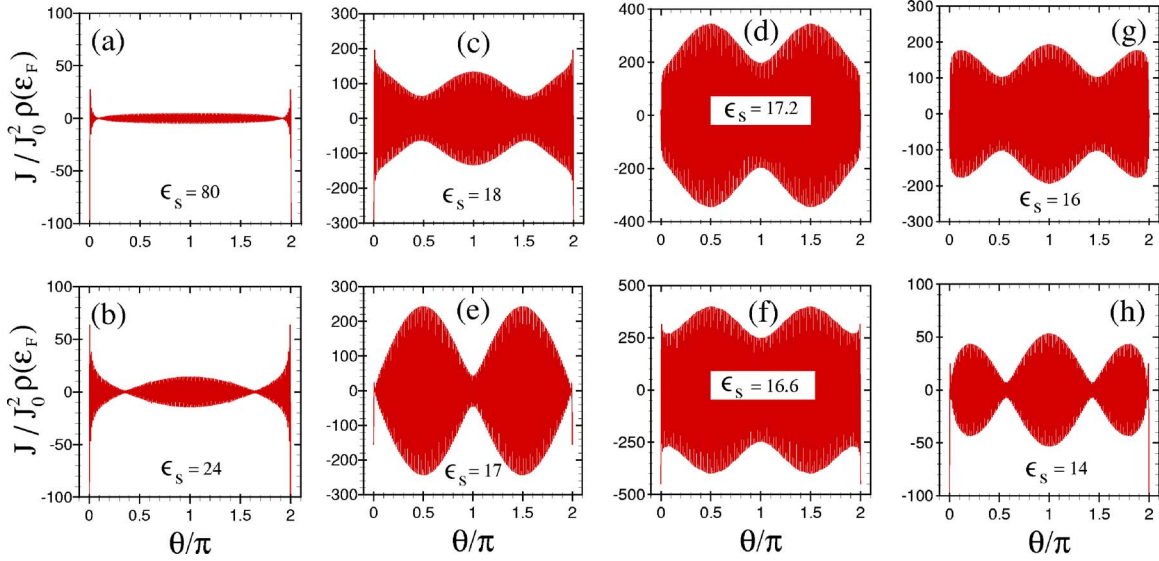


FIG. 8. (Color online) Indirect exchange coupling,  $J$ , vs angular distance,  $\theta$ , between the two nuclear spins in the presence of the external magnetic flux,  $\varphi=0.499$ , for eight dielectric constants,  $\epsilon_s$ . First, (a)  $\epsilon_s=80$ , (b)  $\epsilon_s=24$  and (c)  $\epsilon_s=18$  for  $\epsilon_s > 17.44$ . Next, (d)  $\epsilon_s=17.2$ , (e)  $\epsilon_s=17$ , and (f)  $\epsilon_s=16.6$  for  $16.44 < \epsilon_s < 17.44$ . Finally, (g)  $\epsilon_s=16$  and (h)  $\epsilon_s=14$  for  $14 < \epsilon_s < 16.44$ . The parameters of the ring are  $N=294$  and  $R=10$  nm.

$\Pi^0(n, \varphi)$  do not intersect. But, by decreasing  $\epsilon_s$  the sharp maxima appears at the integer values of  $\varphi$  rather than the half-integer values.

(3) For  $14 < \epsilon_s < 17.44$ , Figs. 6(g)–6(i), there are two kinds of coupling transitions. One occurs at the values of the magnetic flux which are determined by the intersections of the functions  $1/I(n)$  and  $\Pi^0(n, \varphi)$  in Fig. 4(c) and the other occurs at the values of the magnetic flux for which the exchange coupling is zero.

We finally discuss the behavior of the indirect exchange coupling as a function of the angular distance between the two nuclear spins. Our numerical results are been shown in Figs. 7 and 8 for  $\varphi=0$  and  $\varphi \cong 0.5$ , respectively.

For  $\epsilon_s > 26.44$ , we have the normal behavior of the RKKY interaction as seen in Figs. 7(a) and 7(b); i.e., it oscillates with the period  $\theta_{RKKY} = 2\pi/2n_F + 1$  and the amplitude of the oscillations decays with  $1/2n_F + 1$ .<sup>32</sup> Near  $\epsilon_s = 26.44$ , Fig. 3, the static spin response function of the system has a ferromagnetic or antiferromagnetic transition depending on whether we have  $\epsilon_s \rightarrow 26.44^-$  or  $\epsilon_s \rightarrow 26.44^+$ , respectively. In this case, by decreasing  $\epsilon_s$  the behavior of the exchange coupling changes from Fig. 7(c) to Fig. 7(d).

For  $\epsilon_s < 26.44$ , Fig. 3, by decreasing  $\epsilon_s$  the system responds resonantly at the angular quantum numbers  $2n_F$  and  $2n_F + 2$ . Indeed, in this case by decreasing  $\epsilon_s$  the spin-antisymmetric effective potential increases (Fig. 1) and this increases the contribution of other modes close to  $2n_F + 1$  to the RKKY amplitude. The interference of these modes causes the amplitude of the RKKY interaction to acquires an oscillating envelope beside its usual  $2n_F + 1$  oscillation [Figs. 6(e)–6(h)]. These new modes which come from the low values of the denominator of  $\chi^s(n, \varphi)$  in Eq. (37), are mostly due to the resonance behavior of the static spin response function close to  $2n_F + 1$ . Referring to Fig. 3, we see that at the angular quantum numbers  $n_1 = 2n_F = 146$  and  $n_2 = 2n_F + 2$

$= 148$ , maximum response of the system occurs. In this case, the period of the RKKY oscillations is

$$\theta_{RKKY} = \frac{\pi}{R \left( \frac{2\pi}{L} \right) \left( \frac{n_2 + n_1}{2} \right)} = \frac{2\pi}{2n_F + 1} \quad (38)$$

and the period of its envelope curve with  $\epsilon_s$  equal to 14 is

$$\theta_{env} = \frac{\pi}{R \left( \frac{2\pi}{L} \right) \left( \frac{n_2 - n_1}{2} \right)} = \pi. \quad (39)$$

In Fig. 8, we have depicted the three situations (i), (ii), and (iii), mentioned previously. In Figs. 8(a)–8(c) for  $\epsilon_s > 17.44$ , the interference of  $2n_F$  and  $2n_F + 2$  modes causes the amplitude of the RKKY interaction to acquire the oscillating envelope beside its usual  $2n_F + 1$  oscillations similar to Figs. 6(e)–6(h). In Figs. 8(d)–8(f) for  $16.44 < \epsilon_s < 17.44$ , also, the interference of  $2n_F$  and  $2n_F + 2$  modes causes the amplitude of the RKKY interaction to acquire the oscillating envelope beside its usual  $2n_F + 1$ , but in this case the phase of the envelope curve shifts by  $\pi$  because of changing the sign in the static spin response function at  $2n_F$  [Figs. 5(a) and 5(b)]. The period of the envelope curve is  $\theta_{env} = \pi$ .

Finally, in Figs. 8(g) and 8(h), we have depicted the behavior of the RKKY interaction for  $14 < \epsilon_s < 16.44$ . In this case, too, due to the changing sign of the static spin response function from ferromagnetic to antiferromagnetic at  $2n_F + 2$  [Figs. 5(b) and 5(c)], the phase of the envelope curve shifts by  $\pi$  and the spin response of the system for  $2n_F + 2$  is much larger than for  $2n_F$ . There is a competition between  $2n_F$ ,  $2n_F + 1$ , and  $2n_F + 2$  modes with decreasing  $\epsilon_s$ . This causes the period of the envelope curve to be less than  $\pi$ . Also, the amplitude of the RKKY interaction can increase as a function of distance and causes strong coupling between the two

nuclear spins even at far distances on the ring, Fig. 8(h).

In conclusion, our numerical results obtained using the self-consistent method of LST indicate that the electron-electron interaction and the electron spin correlations in mesoscopic metallic rings bring about effects on the behavior of the RKKY interaction that the RPA fails to predict. The failure of RPA can be traced back to the one-dimensionality and the circular geometry of the ring. The one-dimensionality

causes the  $2k_F$  singularity of the spin response function and the circular geometry changes the spectrum from the continuum to the discrete and brings about the interference of the modes on the ring. The interplay between these effects and the effect of the AB flux on the phases of the electron wave functions produce the reach behavior of the exchange coupling on the ring.

\*Email address: eb.heidari@gmail.com

†Email address: ebrahimi@sbu.ac.ir

- <sup>1</sup>S. Das Sarma, J. Fabian, X. Hu, and I. Žutić, *Solid State Commun.* **119**, 207 (2001).
- <sup>2</sup>D. P. DiVincenzo, *Science* **270**, 255 (1995).
- <sup>3</sup>M. A. Nielsen and I. L. Chuang, *Quantum Computation and Quantum Information* (Cambridge University, Cambridge, 2000).
- <sup>4</sup>I. Shlimak, V. I. Safarov, and I. D. Vagner, *J. Phys.: Condens. Matter* **13**, 6059 (2001).
- <sup>5</sup>D. DiVincenzo, *Fortschr. Phys.* **48**, 771 (2000).
- <sup>6</sup>M. Friesen, P. Rugheimer, D. E. Savage, M. G. Lagally, D. W. van der Weide, R. Joynt, and M. A. Eriksson, *Phys. Rev. B* **67**, 121301 (2003).
- <sup>7</sup>X. Hu and S. Das Sarma, *Phys. Rev. A* **61**, 062301 (2000); **64**, 042312 (2001).
- <sup>8</sup>B. E. Kane, *Nature (London)* **393**, 133 (1998); *Fortschr. Phys.* **48**, 1023 (2000).
- <sup>9</sup>B. Koiller, X. Hu, and S. Das Sarma, *Phys. Rev. Lett.* **88**, 027903 (2002); B. Koiller, X. Hu, H. D. Drew, and S. Das Sarma, *ibid.* **90**, 067401 (2003).
- <sup>10</sup>J. Levy, *Phys. Rev. Lett.* **89**, 147902 (2002).
- <sup>11</sup>F. Meier, J. Levy, and D. Loss, *Phys. Rev. Lett.* **90**, 047901 (2003).
- <sup>12</sup>V. Privman, I. D. Vagner, and G. Kventsel, *Phys. Lett. A* **239**, 141 (1998).
- <sup>13</sup>A. J. Skinner, M. E. Davenport, and B. E. Kane, *Phys. Rev. Lett.* **90**, 087901 (2003).
- <sup>14</sup>F. Troiani, E. Molinari, and U. Hohenester, *Phys. Rev. Lett.* **90**, 206802 (2003).
- <sup>15</sup>R. Vrijen, E. Yablonovitch, K. Wang, H. W. Jiang, A. Balandin, V. Roychowdhury, T. Mor, and D. DiVincenzo, *Phys. Rev. A* **62**, 012306 (2000).
- <sup>16</sup>S. Das Sarma, *Am. Sci.* **89**, 516 (2001).
- <sup>17</sup>D. Esteve and D. Vion, cond-mat/0505676 (unpublished).
- <sup>18</sup>Y. V. Pershin and C. Piermarocchi, *Phys. Rev. B* **72**, 245331 (2005).

- <sup>19</sup>Y. V. Pershin, I. D. Vagner, and P. Wyder, *J. Phys.: Condens. Matter* **15**, 997 (2003).
- <sup>20</sup>M. A. Ruderman and C. Kittel, *Phys. Rev.* **96**, 99 (1954).
- <sup>21</sup>T. Kasuya, *Prog. Theor. Phys.* **16**, 45 (1956).
- <sup>22</sup>K. Yosida, *Phys. Rev.* **106**, 893 (1957).
- <sup>23</sup>D. C. Mattis, *The Theory of Magnetism* (Harper and Row, New York, 1965) Chap. 7.
- <sup>24</sup>C. Kittel, *Solid State Physics*, edited by F. Seitz, D. Turnbull, and H. Ehrenreich (Academic, New York, 1968), Vol. 22.
- <sup>25</sup>Y.-X. Liu, L. F. Wei, J. S. Tsai, and F. Nori, *Phys. Rev. Lett.* **96**, 067003 (2006).
- <sup>26</sup>C. Piermarocchi, P. Chen, L. J. Sham, and D. G. Steel, *Phys. Rev. Lett.* **89**, 167402 (2002).
- <sup>27</sup>H. Tamura, K. Shiraishi, and H. Takayanagi, *Jpn. J. Appl. Phys., Part 2* **43**, L691 (2004).
- <sup>28</sup>Y. Utsumi, J. Martinek, P. Bruno, and H. Imamura, *Phys. Rev. B* **69**, 155320 (2004).
- <sup>29</sup>D. Loss and D. P. DiVincenzo, *Phys. Rev. A* **57**, 120 (1998).
- <sup>30</sup>G. Burkard, D. Loss, and D. P. DiVincenzo, *Phys. Rev. B* **59**, 2070 (1999).
- <sup>31</sup>J. Voit, *Rep. Prog. Phys.* **57**, 977 (1994).
- <sup>32</sup>E. B. Kolomeisky and J. P. Straley, *Rev. Mod. Phys.* **68**, 175 (1996).
- <sup>33</sup>J. M. Luttinger, *Phys. Rev.* **119**, 1153 (1960).
- <sup>34</sup>H. J. Schulz, in *Proceedings of Les Houches Summer School LXI* edited E. Akkermans, G. Montambaux, J. Pichard, and J. Zinn-Justin (Elsevier, Amsterdam, 1995), p. 533.
- <sup>35</sup>R. Lobo, K. S. Singwi, and M. P. Tosi, *Phys. Rev.* **186**, 470 (1969).
- <sup>36</sup>R. K. Moudgil, P. K. Ahluwalia, and K. N. Pathak, *Phys. Rev. B* **51**, 1575 (1995).
- <sup>37</sup>B. Tanatar, *Physica B* **228**, 329 (1996).
- <sup>38</sup>A. L. Fetter and J. D. Walecka, *Quantum Theory of Many-Particle Systems* (McGraw-Hill, New York, 1971).
- <sup>39</sup>M. Tas and M. Tomak, *Phys. Rev. B* **70**, 235305 (2004).
- <sup>40</sup>T. M. Mishonov, T. I. Valchev, L. A. Atanasova, and P. A. Ivanov, cond-mat/0301548 (unpublished).